2014

Decomposing Decision Components in the Stop-signal Task: A Model-based Approach to Individual Differences in Inhibitory Control

C. N. White

E. Congdon

J. A. Mumford

K. H. Karlsgodt
Hofstra Northwell School of Medicine

F. W. Sabb

See next page for additional authors

Authors
C. N. White, E. Congdon, J. A. Mumford, K. H. Karlsgodt, F. W. Sabb, N. B. Freimer, E. D. London, T. D. Cannon, R. M. Bilder, and R. A. Poldrack

Published in final edited form as:
J Cogn Neurosci. 2014 August ; 26(8): 1601–1614. doi:10.1162/jocn_a_00567.

Decomposing decision components in the Stop-signal task: A model-based approach to individual differences in inhibitory control

Corey N. White[9], **Eliza Congdon**[2,3], **Jeanette A. Mumford**[1], **Katherine H. Karlsgodt**[4], **Fred W. Sabb**[3], **Nelson B. Freimer**[2,3], **Edythe D. London**[3,5], **Tyrone D. Cannon**[6], **Robert M. Bilder**[3,7], and **Russell A. Poldrack**[1,8]

[1]Department of Psychology, University of Texas at Austin, Austin, TX, USA

[2]Center for Neurobehavioral Genetics, University of California Los Angeles, Los Angeles, CA, USA

[3]Department of Psychiatry, Semel Institute for Neuroscience and Human Behavior, University of California Los Angeles, Los Angeles, CA, USA

[4]Department of Psychiatry, Zucker Hillside Hospital, North Shore-LIJ, Queens, NY, USA

[5]Department of Molecular and Medical Pharmacology, University of California Los Angeles, Los Angeles, CA, USA

[6]Department of Psychology, Yale University, New Haven, CT, USA

[7]Department of Psychology, University of California Los Angeles, Los Angeles, CA, USA

[8]Department of Neurobiology, University of Texas at Austin, Austin, TX, USA

[9]Department of Psychology, Syracuse University, Syracuse, NY, USA

Abstract

The Stop-signal task (SST), in which participants must inhibit prepotent responses, has been used to identify neural systems that vary with individual differences in inhibitory control. To explore how these differences relate to other aspects of decision-making, a drift diffusion model of simple decisions was fitted to SST data from Go trials to extract measures of caution, motor execution time, and stimulus processing speed for each of 123 participants. These values were used to probe fMRI data to explore individual differences in neural activation. Faster processing of the Go stimulus correlated with greater activation in the right frontal pole for both Go and Stop trials. On Stop trials stimulus processing speed also correlated with regions implicated in inhibitory control, including the right inferior frontal gyrus, medial frontal gyrus, and basal ganglia. Individual differences in motor execution time correlated with activation of the right parietal cortex. These findings suggest a robust relationship between the speed of stimulus processing and inhibitory processing at the neural level. This model-based approach provides novel insight into the interrelationships among decision components involved in inhibitory control, and raises interesting

Corresponding Author: Corey N. White, 409 Huntington Hall, Syracuse University, Syracuse, NY, 13244, cnwhite@syr.edu, Phone: 315-443-2950.

questions about strategic adjustments in performance and inhibitory deficits associated with psychopathology.

Keywords

drift-diffusion model; fMRI; Individual differences; inhibitory control; Stop signal task

Introduction

Inhibitory control is an important component of executive function, and it is typically assessed using tasks in which participants must withhold or inhibit a prepotent response. In the Stop-signal task (SST) participants make simple decisions about a visual stimulus, but on some trials a signal is presented after the stimulus indicating that the response is to be withheld (Figure 1). Differences in inhibitory control are often assessed by calculating a stop-signal reaction time (SSRT), which provides an index of how long it takes an individual to inhibit the response, and thus the strength of their inhibitory ability. Differences in SSRT across individuals relate to activation of a number of neural systems involved in the "stopping network", including right inferior frontal gyrus, posterior parietal cortex, and pre-supplementary motor areas (Aron, 2007; Cai et al., 2013; Congdon et al., 2010). Individuals with shorter SSRTs, reflective of stronger/faster inhibition, typically show greater activation of these neural systems on inhibition trials.

A great deal of work has been carried out to investigate the underpinnings of individual differences in inhibitory control and their relation to the neural systems engaged during response inhibition. Understanding how inhibitory control operates is particularly relevant for clinical researchers, as a number of impulse control disorders (including ADHD and drug addiction) have been shown to demonstrate impaired inhibitory control and reduced neural activation of the stopping network in the SST (Alderson et al., 2007; Aron, 2007; Fillmore & Rush, 2006; Lipszyc & Schachar, 2010; Monterosso et al., 2005). Much of the work in this area relies on calculating an SSRT for each individual and using that measure to probe activation on Stop-trials. However, performance in the SST is determined by other aspects of the decision process as well, including the level of caution in responding and the speed of processing the visual Go stimulus. In light of this, we pursued a different approach to understanding individual differences in inhibitory control. We focused on individual differences in decision components based solely on Go trials (when no stop signal is presented), and assessed the degree to which these components were associated with activation of the stopping network on Stop trials. Because relatively little is known about how different aspects of the decision process relate to the neural systems involved in inhibitory control, this endeavor can provide insight into the factors driving individual differences in inhibitory activation.

To explore the relationship between individual differences in decision components and fMRI activation in the SST, a drift-diffusion model of simple decisions (DDM; Ratcliff, 1978) was employed to decompose SST data into psychologically meaningful components. The DDM is a theory of two choice decisions that successfully accounts for both behavioral

and neurophysiological data from simple decision-making tasks (see Methods). The model can be fitted to accuracy values and response times (RTs) from Go trials to extract values corresponding to the speed/strength of stimulus processing, the level of response caution, and the combined time needed for nondecision processes (such as visual encoding and motor execution). An alternative approach would use behavioral measures to directly index the relevant decision component (e.g., faster RTs indicate faster stimulus processing); however, these raw measures reflect contributions from multiple decision components. Slower RTs could be due to poorer stimulus processing, or instead more cautious speed/accuracy settings. In contrast, a DDM analysis separates behavioral effects into distinct psychological components, which can then be mapped independently onto neural activation. In this manner, models like the DDM provide a bridge between brain and behavior, accounting not only for behavioral data, but also for the underlying physiology involved in simple decisions, including single-cell recordings (Gold & Shadlen, 2007) and fMRI BOLD activation (Heekeren et al., 2008). Further, such models have been shown to be more sensitive than behavioral measures in detecting BOLD activation related to cognitive processing (Forstmann et al., 2010; White et al., 2012) and in dissociating behavioral effects from different experimental conditions (White et al., 2010). In light of these advantages over traditional analyses based on RTs or accuracy values, the DDM was fit to SST data from 123 participants, and individual differences in the resulting components were examined in relation to fMRI activation during inhibitory control.

The approach in this study fits the behavioral model to data from Go trials, whereas previous approaches have analyzed responses on Stop trials (i.e., commission errors) or calculated an SSRT to account for processing on Stop trials. The present approach can be thought of as complementary to more traditional analyses with SSRTs, by examining how well individual differences in neural activation can be accounted for by response tendencies on Go trials where no stop signal is presented. These response tendencies were used to assess neural activation for both Go trials and Stop Inhibit trials to determine how they relate to inhibitory control in the presence of the stop signal. The results show that individual differences in inhibition-related neural activation on Stop trials are very strongly related to differences in decision components calculated solely from Go trials, particularly the measure relating to the speed/strength of processing the Go stimulus. In other words, individuals with faster/stronger stimulus processing on Go trials had stronger activation of the stopping network on Stop trials. This relationship suggests that deficits in inhibitory control associated with addiction and other psychopathologies might actually reflect more general deficits that are present even for simple decisions in the absence of inhibitory control.

Methods

Participants

All participants were recruited from the Los Angeles area as part of a larger study within the Consortium for Neuropsychiatric Phenomics at UCLA (www.phenomics.ucla.edu), in which they completed extensive neuropsychological testing and underwent fMRI scanning. The participants, ages 21–50, were recruited by community advertisements from the Los Angeles area. To be included, participants had to be either “White, Not of Hispanic or Latino Origin”

or “Hispanic or Latino, of Any Race” following NIH designations of racial and ethnic minority groups, and have completed at least 8 years of education (other racial and ethnic minority groups were excluded because this was thought to increase risk of confounding planned genetic studies). For participants who spoke both English and Spanish, language for testing was determined by verbal fluency tests in each language. Participants were screened for neurological disease, history of head injury with loss of consciousness or cognitive sequelae, use of psychoactive medications, substance dependence within past 6 months, history of major mental illness, and current mood or anxiety disorder. All subjects underwent a Structured Clinical Interview for DSM-IV (SCID-I; First, Spitzer, Gibbon, & Williams, 2004). Diagnoses followed the Diagnostic and Statistical Manual of Mental Disorders, Fourth Edition – Text Revision (American Psychiatric Association, 2000). A subset of the group participating in cognitive and behavioral assessments also took part in two separate fMRI sessions (order counterbalanced across subjects), which each included one-hour of behavioral testing and a one-hour scan on the same day (which included the Stop-signal task).

Additional exclusion criteria for the scan portion included the following: history of significant medical illness, contraindications for MRI (including pregnancy), vision that was insufficient to see task stimuli, and left-handedness. 139 healthy adults completed at least a portion of the fMRI sessions; of those, 9 were excluded altogether (6 for an unusable MPRAGE, 2 for withdrawing from the study, and 1 for being disqualified) and 7 were excluded from the present Stop-signal analyses (2 for not completing the scan in which Stop-signal was collected, 3 for excessive motion, and 2 for poor task performance (see *Analysis of Behavioral Data* for performance criteria). Data from a total of 123 participants (57 females) was available for Stop-signal analyses. Of these 123 healthy adults, the mean (standard deviation) of age was 31.14 (8.71). After receiving a thorough explanation, all participants gave written informed consent according to the procedures approved by the University of California Los Angeles Institutional Review Board.

Task

A standard Stop-signal task (Figure 1) was employed in the scanner in which participants were shown a series of Go stimuli (left- and rightwards pointing arrows) in the center of the screen and were told to respond with left and right button presses, respectively (Go trials). On a subset of trials (25%), a stop-signal (a 500 Hz tone presented through headphones) was presented a short delay after the Go stimulus appeared and lasted for 250 ms (Stop trials). Participants were instructed to respond as quickly and accurately as possible on all trials, but to withhold their response on Stop trials (on trials with the tone). Participants were instructed that stopping and going were equally important. On Stop trials, the delay of the onset of the Stop-signal, or Stop-signal delay (SSD), was varied such that it was increased after the participant successfully inhibited in response to a stop-signal (making the next stop trial more difficult), and decreased after the participant failed to inhibit in response to a stop-signal (making the next stop trial less difficult). Each SSD increase or decrease was in a 50 ms interval. The SSD values were drawn from two interleaved staircases (or ladders) per block, resulting in 16 trials from each staircase for a total of 32 Stop trials per block. SSD values started at 250 and 350 ms for ladders 1 and 2, respectively, in the first experiment

block. Two staircases were used rather than one to reduce the ability of participants to notice the adjustments in SSD and change their strategy. At the end of the first experimental block, the last SSD time from each staircase was then carried over to be the initial SSD for the second block. This one-up/one-down tracking procedure ensured that subjects successfully inhibited on approximately 50% of inhibition trials. Also as a result, difficulty level is individualized across subjects and both behavioral performance and numbers of Stop Inhibit trials are equated across subjects.

All participants received training on the task in the form of one initial demonstration, consisting of 8 trials (3 of which were Stop trials), before completing two experiment blocks (one outside of the scanner and one while inside of the scanner). Each experiment block consisted of 128 trials, 96 of which were Go trials and 32 of which were Stop trials (16 from Ladder 1, and 16 from Ladder 2), each presented randomly. Participants completed a total of two blocks for a total of 256 trials. All trials started with a 500 ms white fixation cross in the center of the screen and included a 1000 ms fixed response interval. Subjects were allowed to respond at the start of stimulus presentation until the end of the 1000 ms fixed response interval; once the participant responded, the stimulus disappeared from the screen for the remaining response interval, followed by the null period. Jittered null events were imposed between every trial, with the duration of null events sampled from an exponential distribution (null events ranged from 0.5 to 4 s, with a mean of 1 s).

The presentation and timing of all stimuli and response events were achieved using Matlab (Mathworks) and the Psychtoolbox (www.psychtoolbox.org, Brainard, 1997) on an Apple Powerbook. For the experiment block administered in the scanner, each participant viewed the task through MRI-compatible goggles, and responded with his or her right hand on an MR-compatible button box in the scanner.

fMRI acquisition

Data were collected using 3T Siemens Trio MRI scanners (data collection switched to a different scanner during the study, with data from 103 participants collected on Scanner 1 and 20 participants collected on Scanner 2). For the Stop-signal task run, functional T2*-weighted echoplanar images (EPIs) were collected with the following parameters: slice thickness = 4 mm, 34 slices, TR = 2 s, TE = 30 ms, flip angle = 90°, matrix 64 × 64, FOV = 192 mm. Additionally, a T2-weighted matched-bandwidth high-resolution anatomical scan (same slice prescription as EPI) and MPRAGE were collected. The parameters for MPRAGE were the following: TR = 1.9 s, TE = 2.26 ms, FOV = 250, matrix = 256 × 256, sagittal plane, slice thickness = 1 mm, 176 slices. Although these data are part of a larger study, they have not been published elsewhere presently.

Analysis of Behavioral Data

In order to ensure adequate task performance, Stop-signal data were analyzed as previously reported (Congdon et al., 2010, 2012). The mean, median and standard deviation of reaction time (RT) on Go trials were calculated only for Go trials in which participants correctly responded. Stop inhibit trials included only Stop trials on which participants successfully inhibited a response, and Stop unsuccessful trials included only Stop trials on which

participants responded. Average SSD was calculated from SSD values across staircases. SSRT was estimated using the quantile method, which does not require an assumption of 50% inhibition (Band, 2003). In order to calculate SSRT according to this method, all RTs on Go trials were arranged in ascending order, and the RT corresponding to the proportion of failed inhibition was selected. The average SSD was then subtracted from this quantile RT, providing an estimate of SSRT.

Once summary scores were calculated on the data collected during the scan run, a participant that met any of the following criteria were excluded (following Congdon et al., 2012): 1) percent inhibition on Stop trials less than 25% or greater than 75%; 2) percent correct responding on Go trials less than 60%; 3) percent errors (i.e., incorrect direction) on Go trials greater than 10%; and 4) SSRT estimate that was negative or less than 50 ms. Although SSRT is the primary indicator of task performance, mean and standard deviation of RT on Go trials, percent inhibition on stop trials, and percent errors on Go trials were also examined.

DDM fitting

A DDM (Ratcliff, 1978; Ratcliff & Smith, 2004) was fit to each participant's behavioral data from go trials to extract components of psychological processing. The model, shown in Figure 2, assumes that the decision process starts at some point, *z*, between the boundaries, and noisy evidence is accumulated over time until a boundary is reached, signaling a commitment to that response. The decision time is calculated as the time taken to reach a boundary, and the overall response time is equal to the decision time plus a value of nondecision time that accounts for the duration of other processes like encoding and motor execution. A reduced version of the model was fitted to Go trials to provide estimates for the three primary components of the decision process (as there are no RT data from Stop Inhibit trials the model could not be fit to those trials). The primary components of the model are the boundary separation, nondecision time, and drift rate. The boundary separation (*a*) provides an index of response caution (the speed/accuracy tradeoff); wide boundaries indicate a cautious response style that prefers accuracy over speed. The nondecision time (time for encoding and response, *Ter*) provides an index of the duration of nondecision processes, including encoding of the stimulus and execution of the response. Finally the drift rate (*v*) provides an index of evidence from the presented stimulus; higher values of drift rate indicate strong evidence and lead to fast and accurate responses. In this case the drift rate serves as a proxy for the strength of the evidence driving the Go process, which directly affects how quickly and accurately the decision is made.

The standard DDM was adjusted to account for the structure of the Go trials in the Stop signal task. Specifically a 1000 ms deadline was added to the model to allow for omissions on Go trials (see Figure 2). Thus any simulated trial from the model that took longer than 1000 ms was counted as an omission, consistent with the task structure. Accordingly the model was designed to account for the full data set from Go trials, including the proportions of correct, error, and omission trials, as well as the response time distributions for correct and error trials (by definition there are no RTs for omissions).

The model was fit to each participant's data for Go trials with the following four parameters: boundary separation (*a*), drift rate (*v*), nondecision time (*Ter*), and across-trial variability in the starting point of evidence accumulation. The starting point indexes the *a priori* bias for one response over the other, and variability in the starting point accounts for trial-to-trial fluctuations in expectation. Preliminary fits without this variability parameter produced RT distributions that had too little variability compared to the observed data, so the additional parameter was introduced. Comparison models that allowed either variability in drift rate or variability in nondecision time did not provide as good of fit as the selected model. Importantly, the primary model parameters were highly correlated across these different DDMs, suggesting that the choice of variability parameter does not significantly change the interpretation for the main decision components. The subsequent fMRI analyses only focused on the primary parameters representing response caution (boundary separation, *a*), encoding and motor time (nondecision time, *Ter*), and the speed of go processing (drift rate, *v*).

To maximize the number of RTs for each response and provide more robust estimates of the RT distribution shape, left and right responses were collapsed into correct, incorrect, and omission trials. Consequently the starting point of the diffusion model was fixed at *a*/2 for the fits (assuming unbiased responses). Collapsing the data in this manner glosses over any potential biases across participants, however the focus of this study was on macro-level response tendencies. Further collapsing across right/left responses increases the number of observations to provide more stable estimates of model parameters and BOLD activation. We used the χ^2 minimization technique (Ratcliff & Teurlinckx, 2002) based on the quantiles of the RT distribution. For correct responses, the standard quantiles of the RT distribution (.1, .3, .5, .7, .9) were used to compare against the predicted data from the model. Since there were so few errors, only the median quantile (.5) was used for error responses. These RT quantiles were used with the proportion of each trial type (correct, error, omission) to provide the χ^2 fit index, which was minimized by a SIMPLEX routine (Nelder & Mead, 1965). The starting values for the parameters in the search function were boundary separation = 0.14, nondecision time = 270 ms, drift rate =0.35, and variability in starting point = 0.05, which were estimated from fits to the averaged data across participants. The cost function for the total χ^2 calculation was based on the summed χ^2 difference in observed versus predicted response proportions in each quantile for correct and error responses, plus the χ^2 difference between observed and predicted proportion of omissions. The predicted proportion of omissions was calculated by taking the proportion responses in the cumulative distribution function that were longer than 1000ms (to correspond to the deadline in the task). The proportion of omission trials was sufficiently low for each participant that they do not strongly affect the parameter estimation. Nonetheless, they were included in the fitting to capture as much of the data as possible.

Analysis of fMRI data

Analyses were performed using tools from the FMRIB software library (www.fmrib.ox.ac.uk/fsl), version 4.1 (Smith et al., 2004). The first 2 volumes from each scan were discarded to allow for T1 equilibrium effects. For each scan, images for each participant were realigned to compensate for small head movements (Jenkinson & Smith,

2001). Data were spatially smoothed using a 5-mm, full-width-at-half-maximum Gaussian kernel. The data were filtered in the temporal domain using a nonlinear high-pass filter with a 66 s cutoff. A three-step registration process was used in which EPI images were first registered to the matched-bandwidth high-resolution scan, then to the MPRAGE structural image, and finally into standard (Montreal Neurological Institute (MNI)) space, using nonlinear transformations (Andersson et al., 2007b, a).

Standard general linear model (GLM) fitting was conducted for all data from subjects. The following events were modeled after convolution with a canonical double gamma hemodynamic response function: Go, StopInhibit, StopRespond, and nuisance events, which consisted of incorrect Go trials. Null events were not modeled and therefore were used as an implicit baseline. Events were modeled at the time of stimulus (arrow) onset with a duration of 1.5 s. The six motion parameters and temporal derivatives of all regressors were included as covariates of no interest to improve statistical sensitivity. For each subject, StopInhibit-Go, StopInhibit-StopRespond, Go-Null, and Go-StopRespond contrasts were computed.

The output from the subject-specific analyses was then analyzed using a mixed-effects model with FLAME. Higher-level analyses included group-level StopInhibit-Go, and Go-Null, which were then subjected to whole-brain regression analyses using the behavioral measures and DDM values. In order to rule out potential scanner-related differences, we first checked for interactions between the scanner used and behavioral measures and diffusion model parameters. There were no significant interactions between scanner and activation for the contrasts of interest, but nonetheless all subsequent group-level analyses were conducted with scanner added as a covariate.

For the comparisons of primary interest, separate GLMs were created based on the RT measures and DDM parameters. The standard behavioral GLMs included the Go RT values or the SSRT values that were modulated across individuals. These models provide a baseline pattern of activation related to these traditional behavioral measures. The DDM-based GLM instead used all three primary diffusion model parameters modulated across individual, allowing investigation of how the decision components relate to inhibitory processing. Group-level statistics images were thresholded with a cluster-forming threshold of $z > 2.3$ and a cluster probability of $p < 0.05$, corrected for whole-brain multiple comparisons using Gaussian random field theory. The search region included 246,626 voxels. Brain regions were identified using the Harvard-Oxford cortical and subcortical probabilistic atlases, and all activations are reported in MNI coordinates. For visualization of results, statistical maps were projected onto an average cortical surface with the use of multifiducial mapping using CARET software (Van Essen, 2005). For reporting of clusters, we used the “cluster” command in FSL. Anatomical localization within each cluster was obtained by searching within maximum likelihood regions from the FSL Harvard-Oxford probabilistic atlas to obtain the maximum z-statistic and MNI coordinates within each anatomical region contained within a cluster.

Results

Behavioral Data

The tracking version of the SST was successful in ensuring approximately 50% inhibition across subjects. The mean Percent Inhibition was 48.7% (SD = 6.5%). Summary statistics for the behavioral data are shown in Table 1.

DDM Parameters

The best-fitting parameter values from the model were used to probe the fMRI data. The model parameters are only interpretable to the extent that the model successfully describes the data. To ensure that the model accounted for the data, predicted data from the best-fitting parameter values are plotted against observed data for each participant in Figure 3A. The plots show that the model successfully captured the shape (quantiles) of the RT distribution and proportions of correct and omission trials. This correspondence supports the use of the parameter values to inform the fMRI analysis. Figure 3B shows the histograms for the primary parameters, demonstrating significant variability across participants in the values of the decision components. To give a sense of how the DDM parameters relate to each other and other measures of the SST, Table 2 presents the correlation matrix for each measure.

BOLD Data

Results from the GLMs based on the behavioral measures and the DDM parameters are shown in Table 3 and Figure 4. Any voxels that survive statistical thresholding reflect brain regions whose activation varied in relation to individual differences in the modulated regressors, after adjusting for which scanner was used. Contrasts were performed for negative and positive relationships between each measure and BOLD activation for Go and Stop Inhibit trials. However, not all contrasts resulted in above-threshold fMRI activation, so only the contrasts with significant activation are presented below.

RT measures

Figure 4 (panel A) displays regions that showed a negative relationship with mean Go RT across individuals. On Go trials, there was greater activation of left inferior frontal gyrus (IFG) and insula associated with faster Go speed. On Stop Inhibit trials, faster Go speed was associated with greater activation of right Insula, right medial frontal gyrus (MFG), superior frontal gyrus (SFG), anterior cingulate cortex (ACC), and right angular gyrus (AG). Many of these regions have been previously implicated in SST performance (e.g., Aron, 2007), consistent with the present results. Analyses based on SSRT across individuals also revealed activation of regions typically implicated in inhibitory control, including bilateral basal ganglia and right IFG (Figure 4B). These RT analyses demonstrate neural activation that is largely consistent with previous work in this domain. However, these RT measures do not provide information about which specific decision components are being represented in this analysis. Because RTs are affected by response caution, motor execution, and stimulus processing, it is unclear which components are driving these activation patterns. The DDM parameters presented below circumvent this issue by dissociating the contributions of each decision component.

Drift Rates

Results from the drift rate regressor, which provides an index of the strength/speed of processing the Go stimulus, revealed an interesting relationship between Go and Stop trials. When contrasting Go trials to baseline, activation in right frontal pole and left pre-motor area was positively correlated with the drift rate across individuals (Figure 4C). Notably, a similar frontal region also reflected individual differences in drift rate, Go RT, and SSRT on Stop Inhibit trials. The overlap in activation for drift rates and the RT measures on both Go and Stop trials suggests that this frontal activation reflects the strength of the Go process, consistent with the drift rate interpretation from the DDM. Even on trials with a Stop signal, the Go process is engaged, hence the same relationship with drift rate is observed on both Go and Stop trials.

For Stop trials, the drift rates were also positively correlated with activation of several regions shown to be involved in inhibitory control. Notably this includes the similar regions of right IFG and basal ganglia that were correlated with SSRT. Activation of right IFG is associated with stopping in inhibition tasks (e.g., Boehler et al., 2010; Swann et al., 2012), and subcortical regions including the striatum and subthalamic nucleus have been shown to be involved in inhibitory control (Aron & Poldrack, 2006). Further, on Stop trials the drift rates were related to the same SFG/ACC and AG regions that were correlated with Go RT. Activation in SFG/ACC and posterior parietal regions has been shown to correlate with stopping behavior (Aron, 2007; Boehler et al., 2010; Zheng et al., 2008), though the present results suggest that this relationship might also be driven by aspects of the Go processing (see Discussion).

Together these findings imply a strong relationship across individuals between stimulus processing and response inhibition. Individuals who had stronger Go processing, as reflected by drift rates, Go RTs, and activation in frontal pole, also had stronger inhibitory processing, as reflected by SSRTs and activation of the stopping network. Because the drift rate measure from the DDM provides a more precise index of Go processing strength than RTs (which are affected by other aspects of the decision process), a more specific relationship among these systems could be observed.

Nondecision time

Nondecision time (*Ter*) accounts for the duration of processes outside of the decision process, including stimulus encoding and motor execution. Although this parameter reflects both encoding and motor execution, individual differences in nondecision time are more likely to reflect differences in the latter. Response slowing, which is critical for adapting to the different stop signal durations throughout the task, can be accomplished through delaying motor execution (in addition to increasing response caution). Consequently observed differences in nondecision time are more likely to reflect individual differences in motor execution rather than visual encoding, as only the former can be adjusted to improve performance. Across individuals, nondecision time was negatively correlated with activation of right parietal regions, including AG, on Stop Inhibit trials (Figure 4D). Thus when inhibition was successful, slower motor execution was associated with lower activation of parietal cortex. Similar regions of parietal cortex have been found to relate to corticomotor

excitability and delayed responding (Jahfari et al., 2010), consistent with the present findings. Activation in this region was also negatively correlated with mean RT and positively correlated with drift rates. This overlap suggests that both drift rates and nondecision processes contribute to the RT-related activation in right AG. No significant activation was observed for nondecision time on Go trials.

Boundary Separation

The boundary separation parameter provides an index of response caution and the speed/accuracy tradeoff; larger boundary separation indicates a cautious response style that favors accuracy over speed. There was no significant activation corresponding to individual differences in response caution at the accepted statistical threshold.

Discussion

Inhibitory control is an important component of executive function. The results of the present study provide insight into inhibitory and excitatory processing in the Stop-signal task and how they relate to individual differences in neural activation. Using an alternative approach that focused on decision components calculated from Go trials, the results indicate strong relationships between decision processes and inhibitory activation. Contrasts based on drift rate values, which provide a proxy for the strength or speed of Go processing, revealed an interesting relationship between execution and inhibition. Individuals who had a stronger drift rate for Go trials, exhibiting faster and more accurate responses, had greater activation of the right frontal pole and left MFG on Go trials. Activation in the frontal pole could reflect stronger representation of action/response rules (Badre & D'Esposito, 2009) and/or more effective task monitoring (Bechara et al., 2000), both of which could lead to faster and more accurate processing of the Go stimulus. Notably, relationship between drift rate and frontal pole activation was observed both on Go trials and Stop Inhibit trials. Since both trial types involve the initiation of the Go process (Logan & Cowan, 1984), the finding of activation on both trial types supports the link between drift rate and Go processing. In contrast to activation of the frontal pole, activation of left MFG was only detected on Go trials, suggesting it relates to the motor activation occurring when the response is actually executed.

Even more intriguing is the finding that the same drift rate values, calculated independently from data on Go trials, accounted for a large degree of activation of the stopping network on Stop Inhibit trials. Activation of the basal ganglia, right IFG, SFG/ACC, and AG was strongly correlated with individual differences in the strength of the Go process. Each of these regions has been implicated in inhibitory processing (Aron, 2007; Congdon, et al. 2010), and the results here demonstrate a robust relationship between activation of these regions and the strength of stimulus processing: individuals with stronger/faster stimulus processing had stronger recruitment of the inhibitory network on stop trials.

Although SFG/ACC activation is often observed in the SST, the present results suggest that it might not be specific to inhibitory control. On Stop Inhibit trials, individuals with stronger drift rates (and faster Go RTs) showed greater activation in SFG/ACC. But this activation was not significantly related to SSRTs. Many studies with simple choice tasks show greater

SFG/ACC activation for more difficult decisions within a given task (e.g., Brown & Braver, 2005). It is hypothesized that these regions are involved in performance monitoring and conflict detection based on the uncertainty about the outcome of the current choice (e.g., Alexander & Brown, 2011; Brown & Braver, 2005; 2007). In a standard choice task, lower drift rates are associated with harder decisions and more uncertainty, and therefore also greater SFG/ACC activation (White et al., 2012). But the opposite relationship was observed in the SST in this study; higher drift rates correlated with greater SFG/ACC for Stop trials. This discrepancy is likely driven by the different task requirements and how they affect difficulty and conflict. On Stop trials, faster processing of the Go stimulus would mean greater response activation and greater competition with the Stop process. Thus a stronger drift rate would actually increase uncertainty and conflict regarding whether successful inhibition will occur on Stop trials, leading to greater activation of SFG/ACC.

The observed relationship between Go speed and activation of inhibitory systems like IFG and basal ganglia is largely consistent with the assumptions of race models of SST processing (Logan & Cowan, 1984; Boucher et al., 2007; Verbruggen & Logan, 2008; 2009), which assume that performance on Stop trials is determined by the winner of a race between the Go process and the Stop process. In this framework, a fast and accurate Go process, which is reflected by stronger drift rates, must be accompanied by a fast Stop process for inhibition to be successful (see Figure 5). Individuals who have relatively strong drift rates would need to have strong activation of the stopping network in order to obtain an acceptable level of inhibition success. Our findings show precisely this relationship. Importantly this relationship holds for the drift rate measure, but not nondecision time (though see below), or response caution. Although each of these measures relate to the speed of responses on Go trials, only the measure directly related to the speed/strength of stimulus processing for the Go signal correlated with activation of neural systems in the stopping network. Analyses based on the behavioral measure of mean RTs revealed some of this activation, but were not sensitive enough to detect activation of subcortical regions and show the full extent of this relationship. Note also that although these DDM results are consistent with race models, the analyses did not depend on any assumptions about racing processes and were based solely on data from Go trials. In this regard, the observed relationship between decision components calculated on Go trials and inhibitory neural activation on stop trials appears to be a critical component of processing in the SST, and thus needs to be accounted for by any successful model of stop-signal processing.

The observed relationship between Go processing speed and inhibitory activation also raises an interesting question: to what extent are deficits in inhibitory control associated with psychopathology and addiction related to deficits in processing of the Go stimulus? As mentioned above, a slower Go process does not require the same strength of inhibitory control for successful performance in the SST. The present study shows precisely this relationship in a population of healthy participants with no current psychopathology. However, if the same relationship holds for patient populations characterized by substance or behavioral addictions as well, it would suggest that weaker inhibitory control in those populations is related to, if not a consequence of, weaker stimulus processing. In this regard, weaker inhibitory control would be just one component of broader cognitive deficits in these populations, rather than a specific deficit. In support of this, a recent meta-analytic review of

SST performance in children with Attention-Deficit/Hyperactivity Disorder (ADHD) found not only slower SSRTs, but slower and more variable Go RTs for patients relative to controls (Alderson et al., 2007), which is a signature of weaker drift rates (see correlations in Table 2). Future work will be needed to explore how these individual differences are related, but the present study suggests that the deficits observed in these populations might not be specific to inhibition.

The current study also sheds light on potential strategic adjustments to the response process in the SST. In particular, participants can improve the probability of successful inhibition by strategically slowing their responses. This can be accomplished by increasing response caution (trading speed for accuracy) and/or by delaying the motor response once the decision has been reached. Either type of adjustment could presumably reduce the amount of inhibitory control needed to withhold the response. Our results suggest that such strategic adjustments are more related to the motor response than response caution. First, the nondecision time parameter was more strongly correlated than response caution with SSRT (see Table 2). Second, nondecision time correlated with BOLD activation on Stop Inhibit trials, whereas response caution did not. Slower motor execution across participants, as indexed by the nondecision time parameter, was associated with weaker activation of right AG on Stop trials when inhibition was successful. Recent work with repetitive transcranial magnetic stimulation supports this association with motor execution, showing that similar regions of parietal cortex were critical for quickly implementing motor plans based on sensory information (Verhagen et al., 2012).

In contrast to the nondecision time analysis, there was no significant activation relative to the boundary separation parameter, which provides a proxy for response caution. Recent work with models like the DDM implicates premotor areas and the striatum for adjusting levels of response caution in simple choice tasks (Bogacz et al., 2010; Forstmann et al. 2010), but these regions did not show significant activation in the present study. Since participants could increase their level of caution to improve the probability of successful inhibition, the failure to detect any significant relationship between caution and the stopping network is surprising. However in those previous studies response caution was explicitly manipulated within participants, creating a larger and more sensitive contrast than exists in the present data. Regardless, the present results suggest that delayed motor execution is more closely related to inhibition on Stop trials than response caution.

Conceptually there is reason to expect greater strategic shifts in motor execution rather than caution. In the SST, whether or not a response is successfully inhibited depends on the response itself, not the actual decision. That is, determining if the arrow faces right or left does not preclude successful inhibition so long as the corresponding response has not been executed. In this regard, delaying the decision by increasing caution could be less impactful than delaying the response by slowing motor execution. Thus the present results might reflect greater strategic involvement of the latter compared to the former. However, this interpretation hinges on a null effect for boundary separation, so further work will be needed to explore the relationship between response caution and neural activation in the SST.

In summary the results presented herein provide insight into the neural systems underlying individual differences in performance in the SST. The alternative approach of using the DDM on Go trials provides a complementary technique relative to traditional approaches focusing on SSRT estimates. The parameter values provided increased sensitivity for detecting the underlying neural effects, as the DDM analyses showed subcortical activation that was not detected using RTs (see Forstmann et al. 2010 for a similar finding), and improved specificity for interpreting such effects, as effects related to RTs were dissociated into distinct psychological processes. In this regard the DDM parameters provided deeper insight than traditional behavioral measures into the interrelationships among processing components in the SST. Consequently the relationship between execution-related Go processing in the right frontal pole and inhibitory Stop processing in the distributed fronto-subcortical-parietal network could be identified, raising interesting questions about the nature of processing deficits association with psychopathology. Likewise a significant relationship was revealed on Stop Inhibit trials between delayed motor execution and posterior parietal activation, hinting at a potential strategic mechanism for increasing the likelihood of successful inhibition. More generally this work demonstrates the utility of a model-based approach to probing fMRI data, and highlights the importance of accounting for individual differences in decision components when investigating other aspects of cognition.

Acknowledgments

The authors would like to thank Angelica A. Bato and Eric Miller for their assistance with data collection, in addition to the entire CNP testing staff. This work was supported by the Consortium for Neuropsychiatric Phenomics (NIH Roadmap for Medical Research grants UL1-DE019580 (Bilder, PI), RL1MH083268 (Freimer, PI), RL1MH083269 (Cannon, PI), RL1DA024853 (London, PI), and PL1MH083271 (Bilder, PI)).

References

Alderson RM, Rapport MD, Kofler MJ. Attention-Deficit/Hyperactivity disorder and behavioral inhibition: A meta-analytic review of the Stop-signal paradigm. J Abnorm Child Psychol. 2007; 35:745–758. [PubMed: 17668315]

Alexander WH, Brown JW. Medial prefrontal cortex as an action-outcome predictor. Nat Neurosci. 2011; 14:1338–1344. [PubMed: 21926982]

American Psychiatric Association. Diagnostic and statistical manual of mental disorders. 4. Washington, DC: 2000. Text Revision

Andersson, M.; Jenkinson, M.; Smith, SM. FMRIB technical report TR07JA2. 2007a. Non-linear registration, aka Spatial normalisation.

Andersson, M.; Jenkinson, M.; Smith, SM. FMRIB technical report TR07JA1. 2007b. Non-linear optimisation.

Aron AR. The neural basis of inhibition in cognitive control. Neuroscientist. 2007; 13:214–228. [PubMed: 17519365]

Aron AR, Poldrack RA. Cortical and subcortical contributions to Stop signal response inhibition: role of the subthalamic nucleus. J Neurosci. 2006; 26:2424–2433. [PubMed: 16510720]

Badre D, D'Esposito M. Is the rostro-caudal axis of the frontal lobe hierarchical? Nat Rev Neurosci. 2009; 10:295–307. [PubMed: 19277052]

Band GP, van der Molen MW, Logan GD. Horse-race model simulations of the stop-signal procedure. Acta Psychol (Amst). 2003; 112(2):105–142. [PubMed: 12521663]

Bechara A, Damasio H, Damasio AR. Emotion, decision-making, and the orbitofrontal cortex. Cerebral Cortex. 2000; 10:295–307. [PubMed: 10731224]

Boehler CN, Appelbaum LG, Krebs RM, Hopf JM, Woldorff MG. Pinning down response inhibition in the brain – conjunction analyses of the Stop- signal task. Neuroimage. 2010; 52:1621–1632. [PubMed: 20452445]

Bogacz R, Wagenmakers EJ, Forstmann BU, Nieuwenhuis S. The neural basis of the speed-accuracy tradeoff. Trends Neurosci. 2010; 33:10–16. [PubMed: 19819033]

Boucher L, Palmeri TJ, Logan GD, Schall JD. Inhibitory control in mind and brain: an interactive race model of countermanding saccades. Psychol Rev. 2007; 114:376–397. [PubMed: 17500631]

Brainard DH. The Psychophysics Toolbox. Spat Vis. 1997; 10:433–436. [PubMed: 9176952]

Brown JW, Braver TS. Learned predictions of error likelihood in the anterior cingulate cortex. Science. 2005; 307:1118–1121. [PubMed: 15718473]

Brown JW, Braver TS. Risk prediction and aversion by anterior cingulate cortex. Cogn Aff Behav Neurosci. 2007; 7:266–277.

Cai W, Cannistraci CJ, Gore JC, Leung HC. Sensorimotor-independent prefrontal activity during response inhibition. Hum Brain Mapp. 2013

Congdon E, Mumford JA, Cohen JR, Galvan A, Aron AR, Xue G, Miller E, Poldrack RA. Engagement of large-scale networks is related to individual differences in inhibitory control. Neuroimage. 2010; 53:653–663. [PubMed: 20600962]

Congdon E, Mumford JA, Cohen JR, Galvan A, Canli T, Poldrack RA. Measurement and reliability of response inhibition. Front Psychol. 2012:3–37. [PubMed: 22291676]

Fillmore MT, Rush CR. Polydrug abusers display impaired discrimination-reversal learning in a model of behavioral control. J Psychopharmacol. 2006; 20:24–32. [PubMed: 16174667]

First, MB.; Spitzer, RL.; Gibbon, M.; Williams, JB. Structured Clinical Interview for DSM-IV Axis I disorders, Research Version, Patient edition. (SCID-IP). New York: Biometrics Research, New York State Psychiatric Institute; 2004.

Forstmann BU, Anwander A, Schafer A, Neumann J, Brown S, Wagenmakers EJ, Bogacz R, Turner R. Cortico-striatal connections predict control over speed and accuracy in perceptual decision making. Proc Natl Acad Sci USA. 2010; 107:15916–20. [PubMed: 20733082]

Forstmann BU, Brown S, Dutilh G, Neumann J, Wagenmakers EJ. The neural substrate of prior information in perceptual decision making: A model-based analysis. Front Human Neurosci. 2010; 4:40.

Gold JI, Shadlen MN. The neural basis of decision making. Annu Rev Neurosci. 2007; 30:535–574. [PubMed: 17600525]

Heekeren HR, Marrett S, Ungerleider LG. The neural systems that mediate human perceptual decision making. Nat Rev Neurosci. 2008; 9:467–479. [PubMed: 18464792]

Jahfari S, Stinear CM, Claffey M, Verbruggen F, Aron AR. Responding with restraint: what are the neurocognitive mechanisms? J Cognitive Neurosci. 2010; 22:1479–1492.

Jenkinson M, Smith S. A global optimisation method for robust affine registration of brain images. Med Image Anal. 2001; 5:143–156. [PubMed: 11516708]

Lipszyc J, Schachar R. Inhibitory control and psychopathology: a meta-analysis of studies using the stop signal task. J Int Neuropsychol Soc. 2010; 16:1064–1076. [PubMed: 20719043]

Logan GD, Cowan WB. On the ability to inhibit thought and action: A theory of an act of control. Psychological Review. 1984; 91:295–327.

Monterosso JR, Aron AR, Cordova X, Xu J, London ED. Deficits in response inhibition associated with chronic methamphetamine abuse. Drug Alcohol Depend. 2005; 79:273–277. [PubMed: 15967595]

Nelder JA, Mead R. A simplex method for function minimization. Computer Journal. 1965; 7:208–213.

Ratcliff R. A theory of memory retrieval. Psychol Rev. 1978; 85:59–108.

Ratcliff R, Smith PL. A comparison of sequential sampling models for two-choice reaction time. Psychol Rev. 2004; 111:333–367. [PubMed: 15065913]

Ratcliff R, Tuerlinckx F. Estimation of the parameters of the diffusion model: Approaches to dealing with contaminant reaction times and parameter variability. Psychon Bull Rev. 2002; 9:438–481. [PubMed: 12412886]

Smith SM, Jenkinson M, Woolrich MW, Beckmann CF, Behrens TEJ, Johansen-Berg H, Bannister PR, De Luca M, Drobnjak I, Flitney DE, Niazy R, Saunders J, Vickers J, Zhang Y, De Stefano N, Brady JM, Matthews PM. Advances in functional and structural MR image analysis and implementation as FSL. Neuro Image. 2004; 23:208–219.

Swann NC, Weidong C, Conner CR, Pieters TA, Claffey MP, George JS, Aron AR, Tandon N. Roles for the pre-supplementary motor area and the right inferior frontal gyrus in stopping action: Electrophysiological responses and functional and structural connectivity. Neuroimage. 2012; 59:2860–2870. [PubMed: 21979383]

Van Essen DC. A population-average, landmark- and surface-based (PALS) atlas of human cerebral cortex. Neuroimage. 2005; 28:635–662. [PubMed: 16172003]

Verbruggen F, Logan GD. Response inhibition in the stop-signal paradigm. Trends Cogn Sci. 2008; 12:418–424. [PubMed: 18799345]

Verbruggen F, Logan GD. Models of response inhibition in the stop- signal and stop-change paradigms. Neurosci Biobehav Rev. 2009; 33:647–661. [PubMed: 18822313]

Verhagen L, Dijkerman HC, Medenorp WP, Toni I. Cortical dynamics of sensorimotor integration during grasp planning. J Neurosci. 2012; 32:4508–4519. [PubMed: 22457498]

White CN, Mumford JA, Poldrack RA. Perceptual criteria in the human brain. Journal of Neuroscience. 2012 in press.

White CN, Ratcliff R, Vasey MW, McKoon G. Using diffusion models to understand clinical disorders. J Math Psychol. 2010; 54:39–53. [PubMed: 20431690]

Zheng D, Oka T, Bokura H, Yamaguchi S. The key locus of common response inhibition network for no-go and stop signals. J Cogn Neurosci. 2008; 20:1434–1442. [PubMed: 18303978]

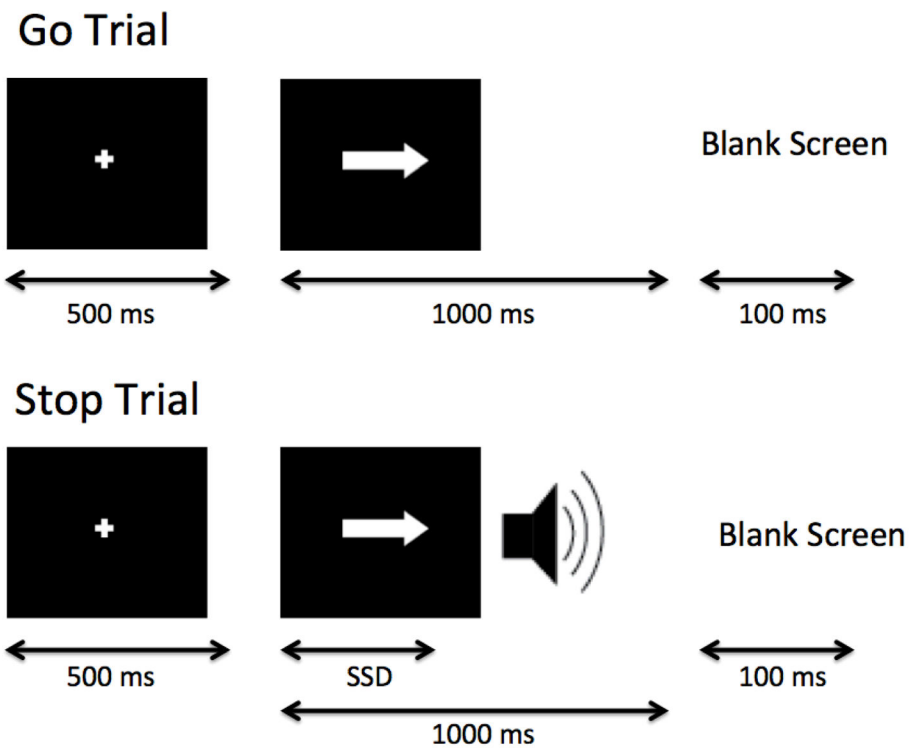

Figure 1.

Schematic of the stop signal task. On Go trials participants must decide if the presented arrow faces right or left and press the corresponding button quickly. On stop trials an auditory stop signal is presented some time after the onset of the arrow (duration indicated by SSD), and participants must withhold their response.

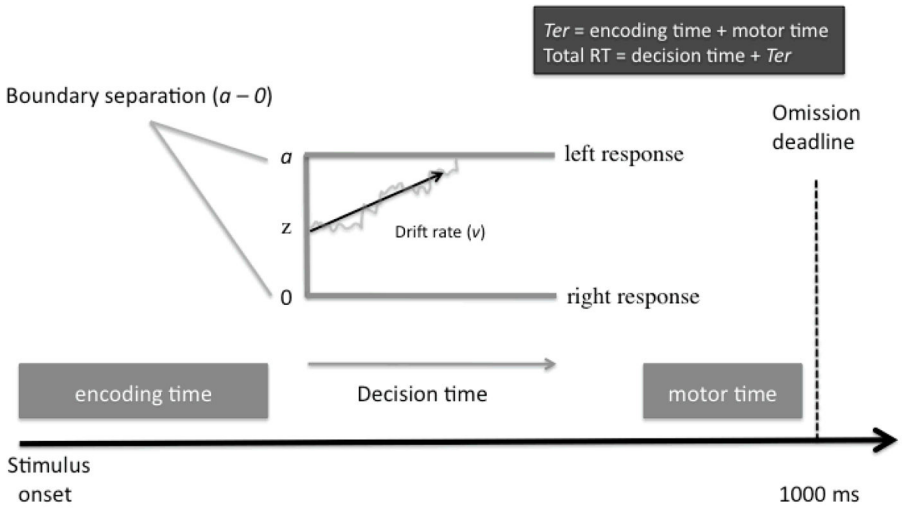

Figure 2.

Illustration of drift-diffusion model for Go trials. The diffusion process accounts for the decision time and is based on the drift rate and boundary separation. The process starts between the boundaries at *z* and drifts until a boundary is reached, corresponding to one of the two decisions (left or right). Drift rate (*v*) indexes the strength or speed of the go process, whereas boundary separation (*a*) indexes the degree of response caution (i.e., speed/accuracy tradeoff, see text). Nondecision time (*Ter*) is calculated as the time taken for processes outside of the decision process (i.e., encoding and motor time). The response time for a trial is equal to the decision time plus nondecision time. The omission boundary at 1000 ms corresponds to the trial duration; any responses longer than the boundary were counted as omissions.

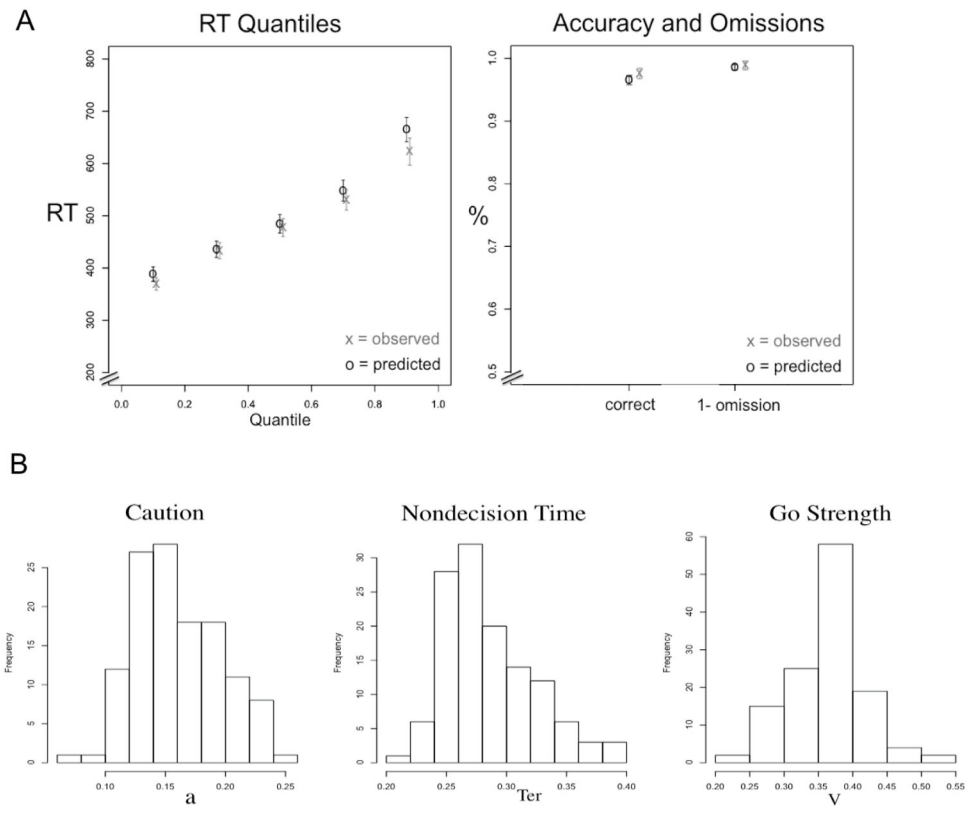

Figure 3.

Results from DDM fitting. A) Fit quality from drift-diffusion model parameters. Values are shown for the quantiles of the RT distributions and proportions of correct and omission responses averaged across participants. Error bars indicate 95% confidence intervals. The results show close correspondence between the observed and predicted values, suggesting the model fit the data well. B) Histograms of primary DDM parameters. Larger values of *a* indicate more cautious responses (slower and more accurate); larger values of *Ter* indicate slower nondecision time; and larger values of *v* indicate stronger excitatory processing on Go trials (faster and more accurate responses).

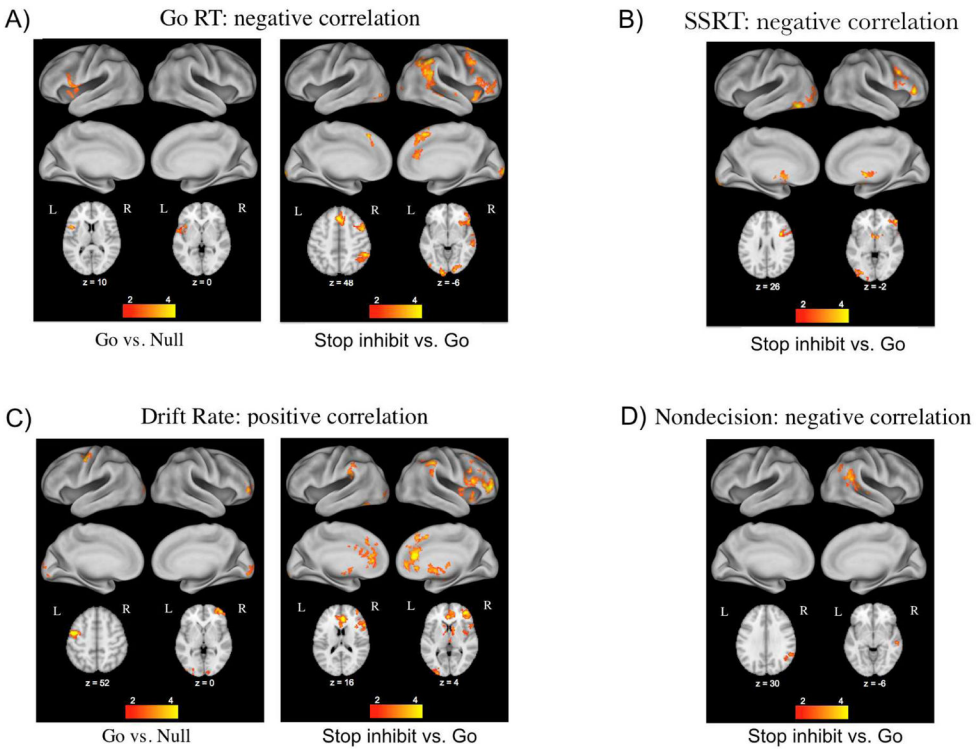

Figure 4.

Neural activation from the GLM analyses. A) Activation relative to individual differences in mean RT. B) Activation relative to individual differences in stop-signal reaction time (note that there was no significant activation for Go vs Null trials). C) Activation relative to individual differences in drift rates (i.e., Go stimulus processing). D) Activation relative to individual differences in nondecision time. Results were corrected for multiple comparisons using cluster-based thresholding ($z = 2.3$, $p < 0.05$).

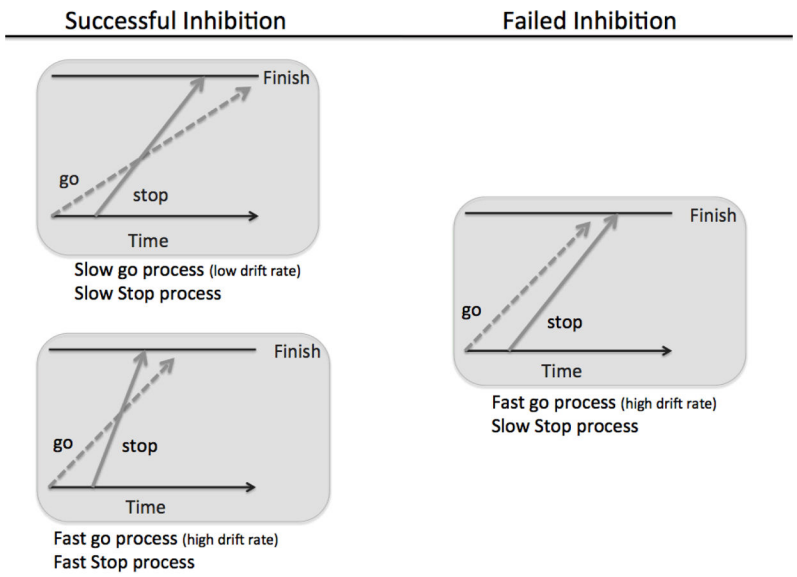

Figure 5.

Schematic of the independent race model. The first process to hit the boundary is the action that is taken (respond or withhold). In the model framework a fast go process must be paired with a fast stop process for successful inhibition (left). If the stop process is too slow, inhibition will fail and many commission errors will occur (right).

Table 1

Summary of Stop-signal task performance in our sample of N = 123. Percent errors in discriminating left and right arrows is given by 1−(percent correct + percent omissions).

Variable	Mean	SD	Minimum	Maximum
SSRT	188.46	57.07	51.89	426.41
Mean Go RT	488.46	96.44	338.48	862.20
SD Go RT	110.02	41.77	43.39	273.77
Percent correct-Go trials	97.59	4.32	65.63	100.00
Percent omissions-Go trials	1.11	3.72	0.00	32.29
Percent inhibition-Stop trials	48.73	6.52	31.25	65.62

Table 2

Correlation matrix for performance measures in the SST. The bottom diagonal presents the correlation coefficient and the top diagonal presents the p-value from each correlation.

	Bound	Nondecision	Drift	Go mean RT	Go RT sd	SSD	SSRT	Percent Inhibition
Bound	--	*0.001*	*0.002*	*< 0.001*	*< 0.001*	*< 0.001*	*0.044*	*0.012*
Nondecision	0.31	--	*<0.001*	*< 0.001*	*< 0.001*	*< 0.001*	*< 0.001*	*< 0.001*
Drift	−0.27	−0.32	--	*< 0.001*	*< 0.001*	*< 0.001*	*< 0.001*	*0.382*
Go mean RT	0.79	0.70	−0.64	--	*< 0.001*	*< 0.001*	*< 0.001*	*< 0.001*
Go RT sd	0.53	0.40	−0.74	0.79	--	*< 0.001*	*< 0.001*	*0.082*
SSD	0.72	0.44	−0.37	0.75	0.50	--	*0.004*	*0.117*
SSRT	0.18	0.35	−0.44	0.40	0.41	−0.26	--	*0.669*
Percent Inhibition	0.23	0.37	−0.08	0.32	0.16	0.14	0.04	--

Bound = boundary separation from DDM; Nondecision = nondecision (encoding and motor) from DDM; Drift = drift rate (speed of go processing) from DDM; SSD = stop-signal duration; SSRT = stop-signal reaction time.

Table 3

Voxels: number of activated voxels per cluster (or region within cluster); z-stat: maximum z-statistic for each cluster; x, y, z are MNI coordinates for the peak of each cluster.

Brain region	Hemisphere	Voxels	Max z-stat	x	y	z
Go vs. Null – RT negative correlation						
IFC/temporal pole	L	627	3.83	−46	10	10
Stop Inhibit vs Go – RT negative correlation						
Occipital Pole/cerebellum	L	2103	4.5	−14	−102	4
SFG/MFG	R	2081	4.73	22	12	64
Supramarginal gyrus/angular gyrus/lateral occipital cortex	R	2032	4.52	56	−48	42
IFC/insula	R	1134	3.96	52	28	−8
Occipital pole/lingual gyrus	R	552	4.12	18	−100	4
Go vs. Null – Drift positive correlation						
Lateral occipital cortex	R/L	1072	3.84	−18	−96	26
Frontal pole	R	652	4.1	44	54	−2
Precentral gyrus/SFG/MFG	L	513	5.16	−42	−4	54
Stop Inhibit vs Go – Drift positive correlation						
Frontal pole/IFC/insula/pallidum/putamen/thalamus*/caudate*/accumbens*	R	3098	4.81	42	48	2
ACC/Paracingulate gyrus/SFG/MFG/subcallosal cortex	R/L	2832	5.21	6	34	18
Supramarginal gyrus/parietal operculum	L	676	4.17	−58	−30	50
Occipital pole	L	541	3.4	−28	−98	4
Supramarginal gyrus/lateral occipital cortex	R	528	3.92	58	−40	46
Inferior temporal gyrus	L	526	3.82	−44	−52	−16
Stop Inhibit vs Go – SSRT negative correlation						
Occipital pole	L	983	4.32	−16	−92	−12
IFC/MFG/temporal pole	R	613	4.02	36	10	26
Caudate/putamen/thalamus/amygdala	R/L	551	3.91	−4	4	2
Lateral occipital cortex/ITG	L	534	4.47	−44	−66	−16
Frontal pole/IFC	R	476	4.72	52	44	2
Stop Inhibit vs Go – Nondecision negative correlation						
Superior and middle temporal gyrus/angular gyrus/lateral occipital cortex	R	838	3.84	56	−36	8

R = right; L = left; SFG = superior frontal gyrus; MFG = middle frontal gyrus; IFC = inferior frontal cortex; ITG = inferior temporal gyrus; ACC = anterior cingulate cortex.